

## Effects of structural microdomains on the vortex correlation length in $a$ -axis oriented $\text{EuBa}_2\text{Cu}_3\text{O}_7$ thin films

E.M. Gonzalez <sup>a</sup>, Z. Sefrioui <sup>b</sup>, B. Maiorov <sup>c</sup>, E. Osquiguil <sup>c</sup>, J. Santamaría <sup>b</sup>, J.L. Vicent <sup>a,\*</sup>

<sup>a</sup> *Departamento Física Materiales, Facultad de Física, Universidad Complutense, 28040 Madrid, Spain*

<sup>b</sup> *GFMC, Departamento de Física Aplicada III, Facultad de Física, Universidad Complutense, 28040 Madrid, Spain*

<sup>c</sup> *Centro Atómico Bariloche, S. Carlos Bariloche, Rio Negro, Argentina*

### Abstract

We have grown  $a$ -axis oriented  $\text{EuBa}_2\text{Cu}_3\text{O}_7$  thin films on  $\text{SrTiO}_3$  (001) substrates using a magnetron sputtering technique. In these films the  $\text{CuO}_2$  planes are aligned parallel to the substrates. The film microstructure shows microdomains. The microdomains are grains with a  $90^\circ$  rotation of the  $c$ -axis. We have done transport measurements in applied magnetic fields up to 16 T. We have found a reduced quasi-2D dimensionality of the vortex glass transition probably resulting of vortex coherence being limited by disorder at domain boundaries. The activation energy for vortex motion in the liquid state displays a  $1/H^{0.5}$  field dependence characteristic of strongly anisotropic superconductor.

© 2005 Elsevier Ltd. All rights reserved.

**Keywords:** A. Superconductors; A. Thin films; B. Epitaxial growth; D. Superconductivity; D. Transport properties

### 1. Introduction

Vortex physics in high temperature superconductors has attracted the attention of many researches during last years. A flood of papers has been published and many different topics have been addressed. Vortices are a very powerful and peculiar tool to study many subjects, which span from phase transitions to soft matter properties. One of the most interesting topics is the role played by the sample itself on the vortex physics. It is well known that many important physical properties show remarkable differences depending on the sample type; for instance, the first order phase transition in single crystals vanishes and becomes a second order phase transition in thin films. The thin film intrinsic defects preclude the first order phase transition and trigger a richer and new scenario.

Some time ago Eom et al. [1] reported the growth of the so-called  $a$ -axis oriented thin films of  $\text{YBa}_2\text{Cu}_3\text{O}_7$  (YBCO) cuprates. In these films the  $\text{CuO}_2$  planes are parallel to the substrate that is the  $a$ -axis lays perpendicular to the substrate. This system seemed very promising, because, for instance, they have longer coherence length perpendicular to the substrate than the usual  $c$ -axis oriented films, this property could be useful to fabricate Josephson junction related devices. Unfortunately, the microdomains induced by the  $\text{SrTiO}_3$

(STO) substrate could be the reason why many researchers feel awkward about these samples. On the other hand, these native microdomains are a very interesting kind of defects. Gonzalez et al. [2] found, in the vortex liquid regime, that the interplay between these extended disorder defects and the vortex phase coherence lengths induce relevant changes in the sample anisotropy and dimensionality.

In this work we have studied the effect of these microdomains on the vortex glass to vortex liquid transition. Magnetic fields up to 16 T have been applied to be sure that the film holds one vortex or more per microdomains. We have found that these native extended disorder defects play a leading role in the properties of the phase transition, because the glass transition is governed by the microdomains boundaries, since the vortex correlation lengths are limited by the microdomain size.

### 2. Experiment

$\text{EuBa}_2\text{Cu}_3\text{O}_7$  (EBCO)  $a$ -axis oriented thin films were grown by dc magnetron sputtering technique in mixed  $\text{Ar}/\text{O}_2$  atmosphere on (100)  $\text{SrTiO}_3$  substrates. The total thickness of the films were 250 nm and the magnetotransport measurements were done using photolithographically patterned bridges with magnetic fields up to 16 T applied perpendicular to the substrates. More details on the films fabrication and characterization could be found elsewhere [3]. The very peculiar microstructure is the most interesting structural property of these samples grown on cubic (100)  $\text{SrTiO}_3$  substrates. High resolution transmission electron microscopy (HRTEM) reveals

\* Corresponding author.

E-mail address: [jlvicent@fis.ucm.es](mailto:jlvicent@fis.ucm.es) (J.L. Vicent).

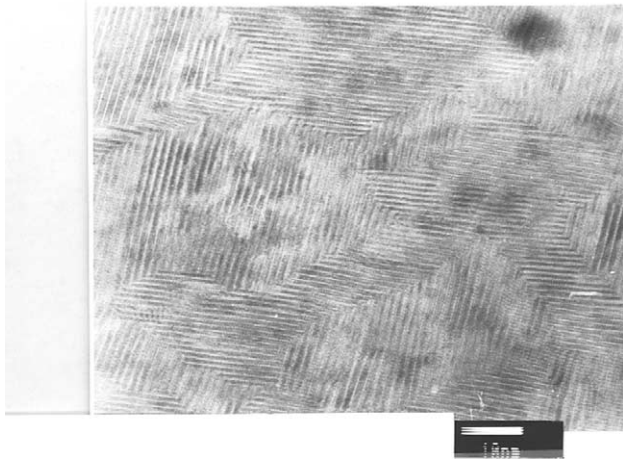


Fig. 1. High-resolution transmission electron microscopy picture of in plane view of  $a$ -axis oriented  $\text{EuBa}_2\text{Cu}_3\text{O}_7$  thin film. The photograph scale is 10 nm.

that EBCO films have microdomains with average size 20 nm. These microdomains have a pure [100] orientation with the  $c$ -axis parallel to the substrate plane, see for instance in Fig. 1 a plan view HRTEM image of an  $a$ -axis oriented thin film. The microdomains are separated by  $90^\circ$  boundaries and the structure at the  $90^\circ$  boundaries is highly coherent [4].

### 3. Results and discussion

Fig. 2 shows the  $R(T)$  transition data at constant magnetic field, applied perpendicular to the substrate, hence parallel to the  $\text{CuO}_2$  planes. These data allow us to extract the first experimental relevant results: the vortex glass transition temperature  $T_g$  and the critical exponent  $s$ . The vortex glass theory [5] explains a straightforward way to obtain  $T_g$ , and the critical exponent  $s$ ; this exponent is the product of the dynamic  $z$  and static  $\nu$  exponents. Their physical means are the divergence of the vortex correlation length at the transition

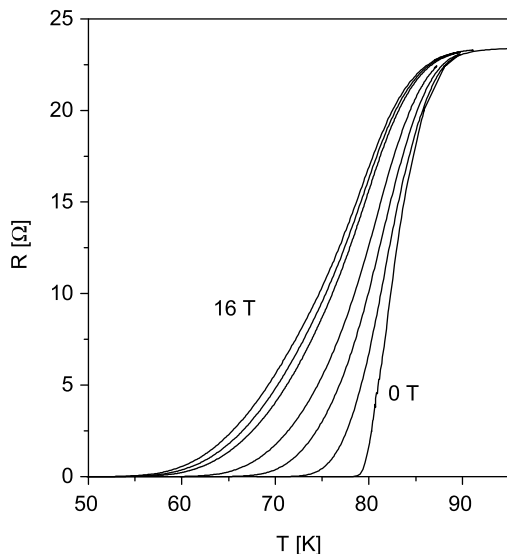


Fig. 2. Resistance vs. Temperature for  $a$ -axis oriented  $\text{EuBa}_2\text{Cu}_3\text{O}_7$  thin film at 0, 1, 3, 6, 12, 14, 6 T from right to left. Magnetic field applied perpendicular to substrate.

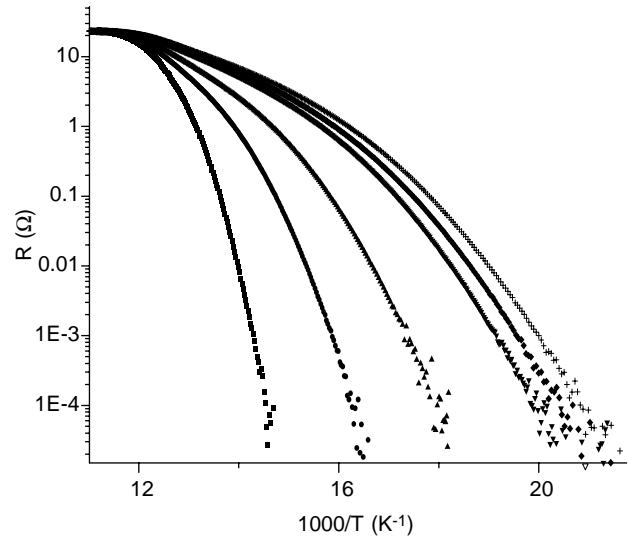


Fig. 3. Log-log plot of Resistance vs.  $1/\text{Temperature}$  for  $a$ -axis oriented  $\text{EuBa}_2\text{Cu}_3\text{O}_7$  thin film at 0, 1, 3, 6, 12, 14, 16 T from right to left.

(given by the value of  $\nu$ ) and the relaxation time divergence (given by the exponent  $s$ ).

The vortex glass model shows the temperature dependence of the linear resistivity  $\rho \sim (T - T_g)^s$ , hence the transition temperature  $T_g$  and the critical exponent  $s$  are obtained from the linear extrapolation to  $(d \ln \rho / dT)^{-1} = 0$  and the inverse of the slope in  $(d \ln \rho / dT)^{-1}$  vs.  $T$ , respectively. Fig. 4 shows the results obtained from the data taken from Fig. 3.

An independent determination of  $T_g$  was done by scaling of  $(I, V)$  curves. Besides this analysis allows going deeper in the nature of the glass transition. Fig. 5(a) shows the rough data and Fig. 5(b) the collapse  $\rho$ - $j$  curves onto a single master curve for temperatures within the critical region. The vortex-glass phase transition was analyzed using the scaling relation [5].

$$E(J) \sim J \xi_g^{D-2-z} E_{\pm} [J \xi_g^{D-1} \phi_0 / K_B T] \quad (1)$$

where  $\xi_g \sim |T - T_g|^{-\nu}$  is the vortex-glass correlation length,  $D$  is the dimension of the system, and  $E_{\pm}$  is a universal scaling

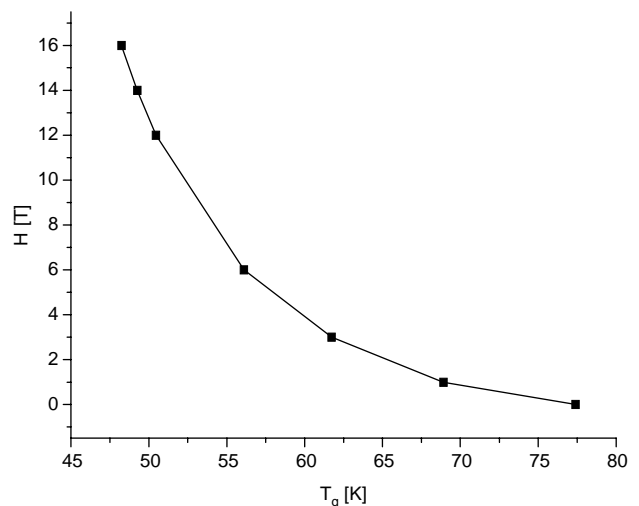


Fig. 4. Vortex glass transition temperature vs. applied magnetic field in  $a$ -axis oriented  $\text{EuBa}_2\text{Cu}_3\text{O}_7$  thin film.

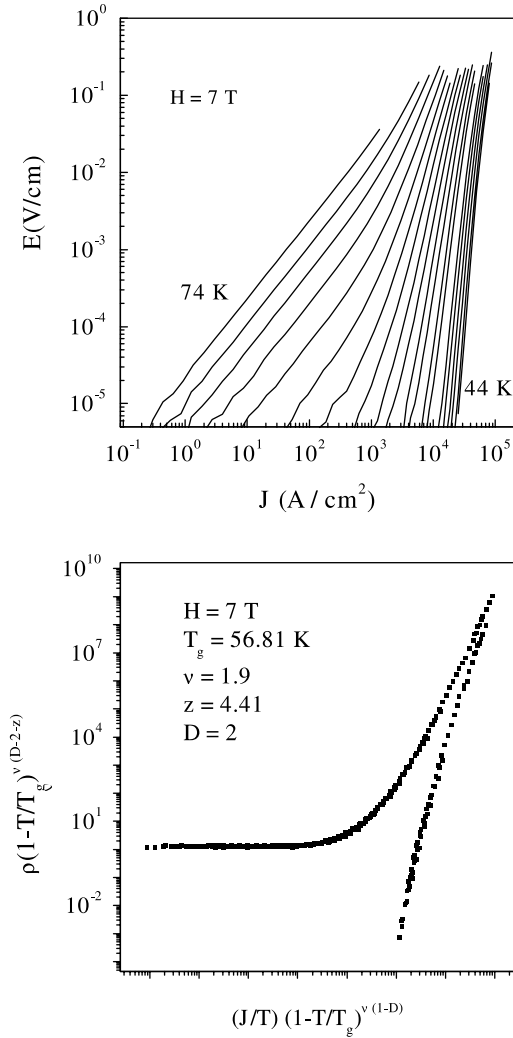


Fig. 5. (a)  $E$ – $J$  characteristics in log–log plot for an  $a$ -axis oriented  $\text{EuBa}_2\text{Cu}_3\text{O}_7$  film in a magnetic field of 7 T. The temperature ranges are from 44 K (lower right) to 74 K (upper left). (b)  $\rho^* - j^*$  scaling curves according to a quasi 2D vortex glass transition, critical exponents were  $z = 4.40 \pm 0.2$ ,  $\nu = 1.9 \pm 0.1$  and  $T_g = 56.81$  K.

function above ( $E_+$ ) and below ( $E_-$ ) the glass transition temperature,  $T_g$ . Electric field data,  $E(j)$ , collapse into two universal scaling functions by plotting data in terms of reduced variables  $\rho^*$  and  $J^*$  defined as:  $\rho^* = \rho(1 - T/T_g)^{\nu(D-2-z)}$  and  $J^* = (J/T)(T - T_g)^{\nu(1-D)}$ . Fig. 5(a) shows the electric field–current ( $E$ – $J$ ) curves in a magnetic field of 7 T applied perpendicular to the substrate (parallel to the  $c$ -axis) and the scaling curve according to Eq. (1). The upper branch of the master function shows a clear positive curvatures resulting from the onset of the non linear regime, the negative curvature of the bottom branch in the high current regime, can be ascribed to the glass phase for which resistivity displays a dependence on current in the form  $\exp[-(j_0/j)^\mu]$  with a positive value of the exponent  $\mu$ . Scaling in terms of a 3D vortex glass transition led to unrealistically high values of the  $z$  critical exponent  $z = 8.5$ ,  $z$  is predicted to be in the range of 4–6 [5]. However, as we can see below an analysis in terms of quasi-2D transition produced reasonable values of the critical

exponents. The exponent  $\mu$  becomes very small when the temperature is approaching  $T_g$  and the slope of the critical isotherm follows

$$\rho(j, T_g) \sim j^\alpha, \tag{2}$$

Therefore we have the possibility of obtaining  $z$  (independent of scaling), since  $\alpha = (z + 2 - D)/(D - 1)$ . The zero extrapolation of  $(d \ln \rho/dT)^{-1}$  plots leads to  $T_g = 56.8$  K, and  $\alpha = 4$ . If we interpret the result as 3D vortex-glass transition, i.e.  $D = 3$ , we obtain an unreasonable high value of  $z = 8.5 \pm 0.2$ . However, assuming a quasi-two-dimensional vortex glass transition with  $D = 2$ ,  $z = 4.4 \pm 0.2$  is obtained, well in the range of variation for  $\alpha$ . This parameters ( $z = 4.4 \pm 0.2$ ,  $\nu = 1.9 \pm 0.1$ ) were used to obtain the good scaling depicted in Fig. 5(b).

The existence of the quasi-2D vortex glass transition can be discussed in terms of the microdomain structure of the  $a$ -axis oriented samples. Since the domains are in the 20 nm ranges, vortex correlations may be broken by domain boundaries. The strong anisotropy of these materials is responsible for the divergence of the vortex glass correlation length  $\xi_g$  near  $T_g$  resulting from the divergence of the individual correlation lengths parallel and perpendicular to the  $c$ -axis ( $\xi_c$  and  $\xi_{ab}$  respectively). Yamasaki et al. [6], have proposed that in the case of a quasi-2D vortex glass transition in Bi based cuprates, a reduced vortex length resulting from the high anisotropy makes  $\xi_c$  to remain practically constant. The divergence of  $\xi_g$  is then restricted to  $\xi_{ab}$ . This is most likely the case of the  $a$ -axis oriented films, in which the divergence of the correlation length in the substrate plane is limited by the boundaries of the microdomains. For this reason,  $a$ -axis oriented EBCO films show a quasi-2D vortex glass transition in a weak anisotropic system, as is the 123 cuprate family.

Finally, the thermally activated form could describe the resistivity in the liquid state

$$\rho(H, T) = \rho_0 \exp[-U(H, T)/k_B T] \tag{3}$$

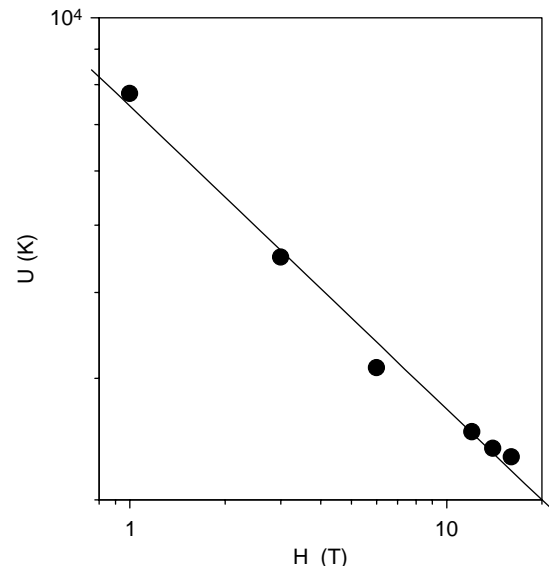


Fig. 6. Log–log plot of activation energy vs. applied magnetic field. The solid line is a fit to  $U \sim H^{-0.5}$ , for an  $a$ -axis oriented  $\text{EuBa}_2\text{Cu}_3\text{O}_7$  film.

where  $U(H,T)$  is the activation energy for vortex motion. From the experimental resistivity data we can extract the magnetic dependence of the activation energy that is depicted in Fig. 6.

The most striking result is the activation energy  $H^{-0.5}$  dependence in the whole applied magnetic range. According to quite a few reports taken from very different systems [7–9], this activation energy behavior is an indication of strong vortex entanglement.

In summary, the vortex glass transition in  $a$ -axis oriented 123 cuprate films deviates from the typical behavior of the usual  $c$ -axis oriented system. The  $90^\circ$  boundaries of the microdomains in  $a$ -axis oriented films induce a quasi-2D behavior, with critical exponents in the usual values and independent of the applied magnetic fields. Moreover in the liquid phase  $a$ -axis oriented 123 films show a strong vortex entanglement.

### Acknowledgements

We want to thank Spanish Ministerio Educación y Ciencia for financial support (MAT2002-04543 and MAT 2002-2642),

'Ramón Areces' Foundation and Argentina CONICET. One of us EMG wants to thank Ministerio de Educación y Ciencia for a Ramón y Cajal contract.

### References

- [1] C.B. Eom, A.F. Marshall, S.S. Laderman, R.D. Jacowitz, T.H. Geballe, *Science* 249 (1990) 1549.
- [2] E.M. Gonzalez, J.M. Gonzalez, J.L. Vicent, *Phys. Rev. B* 62 (2000) 8707.
- [3] M. Velez, J.I. Martín, J.L. Vicent, *Appl. Phys. Lett.* 65 (1994) 2099.
- [4] C. Ballesteros, M.E. Gomez, J.I. Martín, M. Velez, P. Prieto, J.L. Vicent, *Thin Solid Films* 373 (2000) 113.
- [5] D.S. Fisher, M.P.A. Fisher, D.A. Huse, *Phys. Rev. B* 43 (1991) 130.
- [6] H. Yamasaki, K. Endo, S. Kosaka, M. Umeda, S. Yoshida, K. Kajimura, *Phys. Rev. B* 50 (1994) 12 959.
- [7] V.M. Vinokur, M.V. Feigel'man, V.B. Geshkenbein, A.I. Larkin, *Phys. Rev. Lett.* 65 (1990) 259.
- [8] T. Puig, X. Obradors, *Phys. Rev. Lett.* 84 (2000) 1571.
- [9] Z. Sefrioui, D. Arias, E.M. Gonzalez, C. Leon, J. Santamaría, J.L. Vicent, *Phys. Rev. B* 63 (2001) 0645503.